Nonstandard dielectric response

L. Ridgway Scott *

September 22, 2010

Abstract

We compare a nonlinear model for the dielectric effect with a standard discontinuous dielectric model. We also compare both with a discontinuous dielectric model which has an intermediate value in a region between the low dielectric and high dielectric regions in the standard model. These results demonstrate that predictions of the electrostatic environment near the surface of a protein depend strongly on the behavior of the dielectric near the surface.

Continuum models of dielectric solvents surrounding molecules are essential components in predictions of structural conformation and protonation states [1, 15, 22, 28]. These models often are required to estimate the change in electrostatic energy due to a change in charge at a single point at the surface of a protein, e.g., in hydrogen exchange experiments [1, 15, 28]. However, the standard dielectric has a discontinuity at the protein boundary, thus making such estimates delicate.

There is continuing research to identify the proper dielectric model. Several models have been proposed to account for aspects of the dielectric effect that go beyond the original model of Debye [11, 22]. Two different effects near a protein surface lead to suggestions for improvement to the basic bulk dielectric model. The finite size of dielectric molecules implies that they have reduced response to high-frequency electric fields, leading to proposals for what is generally known as a nonlocal dielectric model [4, 5, 6, 7, 8, 9, 10, 12, 20, 23, 24, 25, 26, 32]. Such effects are seen even on the subatomic scale related to electronic polarization [18, 27]. Such high

*The University of Chicago, Chicago, Illinois 60637, email: ridg@uchicago.edu

frequencies can be caused by two effects. In the directions parallel to the protein surface, large electric gradients near the surface are caused by charged and polar sidechains. The scale of these changes in sign in polar sidechains can be on the order of an Ångstrom. In the direction normal to the surface, the rapid change in dielectric also causes potential high-frequencies (e.g., for a discontinuous dielectric, the component of the electric field normal to the surface will be discontinuous).

Similarly, large electric gradients near the surface could cause saturation of the dielectric effect, leading to nonlinear models of the dielectric coefficient [2, 3, 13, 19, 21, 24, 31, 33]. Proximity to hydrophobic groups on a protein surface reduce water mobility and thus would tend to reduce the dielectric effect in addition to these two effects, leading to a need to make the dielectric coefficient dependent as well on proximity to the protein surface.

Models that involve variable dielectric coefficient approximations have been proposed [29, 30, 35]. Approximations have also been proposed in which a nonlocal dielectric coefficient is used in the solvent and a local dielectric coefficient is used in the protein [16, 17, 34].

Another reason for modifying the basic Debye model has to do with the behavior of an ionic solvent surrounding a protein [14]. We will ignore this here. That is, we are considering only the dielectric, and not the ionic, effect.

1 Nonlinear versus nonlocal models

The dielectric effect can be easily described as follows. We consider a system of charge distributions ρ and γ in which the former is based on fixed charged groups but the latter is based on charged groups (with net zero charge) that are free to rotate. The resulting electric potential ϕ satisfies

$$\Delta\phi = \rho + \gamma, \tag{1}$$

where for simplicity we have assumed that the dielectric constant of free space is set to one. We can write $\phi = \phi_\rho + \phi_\gamma$, where for example

$$\Delta\phi_\gamma = \gamma. \tag{2}$$

The ansatz of Debye [11] was that the electric field $E_\gamma = \nabla\phi_\gamma$ should be (on average) parallel to (opposing) the resulting electric field $E = \nabla\phi$:

$$\nabla\phi_\gamma = (1-\varepsilon)\nabla\phi. \tag{3}$$

Taking the divergence of (3) and using (1), we find

$$\Delta\phi_\gamma = \Delta\phi - \nabla\cdot(\varepsilon\nabla\phi) = \rho + \gamma - \nabla\cdot(\varepsilon\nabla\phi). \tag{4}$$

From (2), we thus find

$$\nabla\cdot(\varepsilon\nabla\phi) = \rho. \tag{5}$$

The interpretation of ε can be quite general. The manipulations leading to (5) remain valid when we think of ε as an operator, even a nonlinear one.

It is known that a very good approximation is obtained in bulk water by the assumption that ε is just a constant factor. The model

$$\varepsilon \approx 87.74 - 40.00\,\tau + 9.398\,\tau^2 - 1.410\,\tau^3, \tag{6}$$

where $\tau = T/100$ and T is the temperature in Centigrade (for $T > 0$), is supported by extensive experiments for liquid water [14]. Note that the formula (6) is only intended to apply for water, hence $\tau \in [0, 1]$. This result is remarkable for many reasons. First of all, the fact that ε is much greater than one is surprising, because this means that the strength of the opposing field $E_\gamma = \nabla\phi_\gamma$ is much greater than the field that induces it. It is also surprising that ε increases with decreasing temperature. When water freezes, it increases further: for ice at zero degrees Centigrade, $\varepsilon \approx 92$. But this model cannot hold when the spatial frequencies of the electric field $\nabla\phi$ are commensurate with the size of a water molecule, since the water molecules cannot orient appropriately to align with the field. Thus frequency-dependent versions of ε have been proposed, and these are often called 'nonlocal' models since the operator ε must be represented either as a Fourier integral (in frequency space), or as an integral in physical space with a nonlocal kernel [8, 32].

Nonlinear models arise because the polarization field $\nabla\phi_\gamma$ in the relationship (3) cannot continue to increase indefinitely for $\nabla\phi$ arbitrarily large. The field $\nabla\phi_\gamma$ is due to the fortuitous orientation of the solvent charge groups (e.g., water molecules), but once perfect alignment is achieved, no more improvement can result. (There is an additional effect due to the polarization of the electron distribution of the individual solvent charge groups, but this also will saturate with sufficiently large field strength.) We can write this saturation property mathematically by taking a limit in (3), viz.,

$$\lim_{|\nabla\phi|\to\infty}(1-\varepsilon)\nabla\phi = \lim_{|\nabla\phi|\to\infty}\nabla\phi_\gamma = C, \tag{7}$$

for some constant C depending only on the direction of $\nabla\phi$. Let us write ε as a function of $\nabla\phi$ by introducing a vector $\xi = \nabla\phi$. Then (7) becomes

$$\lim_{|\xi|\to\infty} (1 - \varepsilon(\xi))\xi = C. \tag{8}$$

This constant can potentially depend on the direction of approach to infinity for a simple lattice, but in general it will be isotropic. The value of C can be estimated by considering the case of perfect alignment of water molecules. The dipole of water is 1.85 Debye, and the (maximum) density of water corresponds to about one water molecule per 30 Ångstroms cubed (Å^3), corresponding to a box of side 3.1 Ångstroms. A more intuitive measure of dipole strength is q_e–Å, where q_e is the charge of an electron. Thus the dipole of water is 0.386 q_e–Å. Thus the maximum strength of the water dipole in bulk is about $0.04 q_e$–Å^{-2}.

One simple model that satisfies (8) is

$$\varepsilon(x) = \varepsilon_0 + \frac{\varepsilon_1}{1 + \lambda|\nabla\phi(x)|} \tag{9}$$

for some constants ε_0, ε_1, and λ. We will examine the model (9) in some detail, but we do not intend to suggest it as a serious model. Rather it should be viewed as a prototype nonlinear dielectric model, one that can be easily analyzed and implemented in existing codes for the purposes of software verification.

Both the nonlocal and nonlinear models of the dielectric response have the effect of representing frequency dependence of the dielectric effect. The gradient $|\nabla\phi(x)|$ provides a proxy for frequency content, although it will not reflect accurately high-frequency, low-power electric fields. Thus a combination of nonlocal and nonlinear models for the dielectric response might need to be used in general to capture the full effect.

2 The standard model

We first describe the standard model and give an example of how the solutions behave in a simple geometry. We consider the case when a point charge is at the center of a spherical cavity which contains one material (e.g., protein) surrounded by a dielectric solvent, as depicted in Figure 1(a). The standard

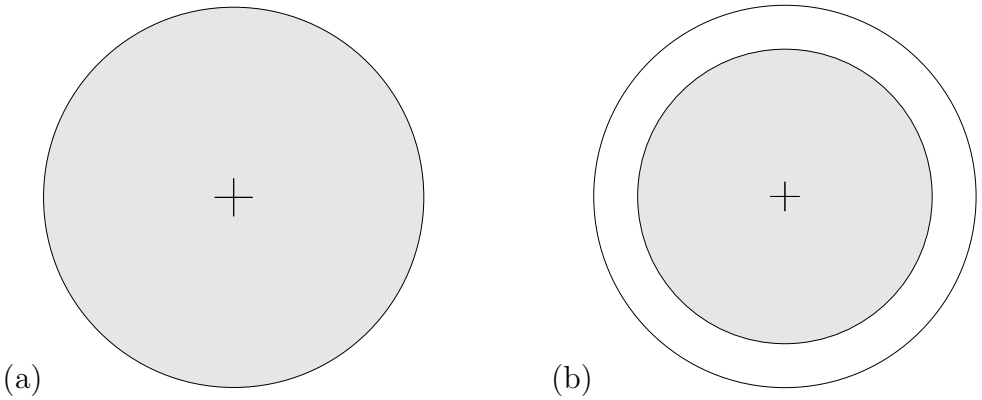

Figure 1: Schematics of a point charge at the center of a spherical cavity having a different dielectric properties from the surrounding dielectric. In (a), the dielectric outside the sphere will be nonlinear. In (b), we consider a piecewise constant dielectric, with the smallest value inside the smaller sphere, and the largest value outside the largest sphere.

dielectric model supposes that

$$\varepsilon_0(x) = \begin{cases} \epsilon_0 & |x| \leq 1 \\ \epsilon_b & |x| > 1, \end{cases} \tag{10}$$

where ϵ_0 could be chosen to be one, and then ϵ_b for water would be about 80, cf. (6). Using the techniques developed in Section 4, we can see that the resulting electrostatic potential ϕ_0 is spherically symmetric and given by

$$\phi_0(r) = \begin{cases} \frac{1}{\epsilon_0 r} + \frac{1}{\epsilon_b} - \frac{1}{\epsilon_0} & r \leq 1 \\ \frac{1}{\epsilon_b r} & r > 1, \end{cases} \tag{11}$$

where $r = |x|$. The main point to note is that the dielectric effect on the potential is local. On either side of the jump, the potential variation is governed by the value of the dielectric; there is no transition zone. Thus the estimate $\varepsilon \approx \epsilon_b$ in the dielectric solvent region governs the value of the potential on the boundary $\{x \in \mathbb{R}^3 : |x| = 1\}$, as well as the gradient of ϕ (the electric field) up to the boundary. Thus if the estimate $\varepsilon \approx \epsilon_b$ is wrong, the predictions of the electrostatics near the boundary will be wrong. We will see by just how much in Section 4.

To get an indication how a local dielectric change can effect the potential, we depict in Figure 1(b) a scenario where there are three values of dielectric:

$$\varepsilon_d(x) = \begin{cases} \epsilon_0 & |x| \le 1 \\ \epsilon_1 & 1 < |x| \le 1+\alpha \\ \epsilon_b & |x| > 1+\alpha \end{cases}, \tag{12}$$

where ϵ_1 is a third value intermediate between ϵ_0 and ϵ_b, and α is the thickness of the intermediate dielectric layer. The resulting electrostatic potential ϕ_d is given by

$$\phi_d(r) = \begin{cases} \frac{1}{\epsilon_0 r} - \frac{1}{\epsilon_0} + \frac{1}{\epsilon_1} + \frac{1}{(1+\alpha)\epsilon_b} - \frac{1}{(1+\alpha)\epsilon_1} & r \le 1 \\ \frac{1}{\epsilon_1 r} + \frac{1}{(1+\alpha)\epsilon_b} - \frac{1}{(1+\alpha)\epsilon_1} & 1 < r \le 1+\alpha \\ \frac{1}{\epsilon_b r} & r > 1+\alpha. \end{cases} \tag{13}$$

Thus we see that the electric field $\nabla\phi_d$ depends only on the chosen dielectric constants in each part of the domain. The value of the potential $\phi_d(1)$ on the inner boundary is given by

$$\phi_d(1) = \frac{1}{\epsilon_1} + \frac{1}{(1+\alpha)\epsilon_b} - \frac{1}{(1+\alpha)\epsilon_1} = \frac{1}{(1+\alpha)\epsilon_b} + \frac{\alpha}{(1+\alpha)\epsilon_1}, \tag{14}$$

so that (11) implies

$$\begin{aligned} \frac{\phi_d(1)}{\phi_0(1)} &= \frac{1}{1+\alpha}\left(1+\alpha\frac{\epsilon_b}{\epsilon_1}\right) \approx (1-\alpha)\left(1+\alpha\frac{\epsilon_b}{\epsilon_1}\right) \\ &\approx 1+\alpha\left(\frac{\epsilon_b}{\epsilon_1}-1\right), \end{aligned} \tag{15}$$

for small α.

3 Nonlinear model: point charge

It is revealing to know the behavior of a dielectric model for a point charge completely surrounded by a bulk dielectric solvent [32]. The isolated charge structures the solvent, and thus reduces its capacity to provide as strong a dielectric effect locally. The extent of the region of reduced effect is not

known precisely, but for water it is expected to be on the order of a few nanometers. We thus consider the model

$$\epsilon(x) = \epsilon_0 + \frac{\epsilon_b - \epsilon_0}{1 + \lambda|\nabla\phi(x)|}, \tag{16}$$

where we can think of ϵ_0 as either the dielectric coefficient of free space, or the dielectric coefficient of some pervasive medium, and we think of ϵ_b as the dielectric coefficient of the bulk solvent.

We seek the potential ϕ for a point (negative) charge at the origin, of strength -4π. Then the equation for ϕ is

$$-\nabla \cdot \left(\left(\epsilon_0 + \frac{\epsilon_b - \epsilon_0}{1 + \lambda|\nabla\phi(x)|} \right) \nabla\phi \right) = 4\pi\delta. \tag{17}$$

We can express this variationally as

$$\int_{\mathbb{R}^3} \left(\epsilon_0 + \frac{\epsilon_b - \epsilon_0}{1 + \lambda|\nabla\phi(x)|} \right) \nabla\phi \cdot \nabla v \, dx = 4\pi v(0) \tag{18}$$

for all sufficiently smooth v with compact support. Since ϕ is spherically symmetric, this reduces to

$$\int_0^\infty \left(\epsilon_0 + \frac{\epsilon_b - \epsilon_0}{1 + \lambda|\phi'(x)|} \right) \phi' v' r^2 \, dr = v(0), \tag{19}$$

provided v is spherically symmetric. The equation

$$\int_0^\infty uv' \, dr = v(0) \tag{20}$$

is solved by $u \equiv -1$, and thus we have

$$-\left(\epsilon_0 + \frac{\epsilon_b - \epsilon_0}{1 + \lambda|\phi'(r)|} \right) \phi'(r) = \frac{1}{r^2}. \tag{21}$$

We can write this as

$$f(\phi'(r)) = -\frac{1}{r^2}, \tag{22}$$

where the function f is defined by

$$f(\xi) = \left(\epsilon_0 + \frac{\epsilon_b - \epsilon_0}{1 + \lambda|\xi|} \right) \xi, \tag{23}$$

where here $\xi \in \mathbb{R}$. Note that

$$f(-\xi) = -f(\xi) \tag{24}$$

for any real ξ. Such antisymmetry thus holds for the inverse function:

$$f^{-1}(-y) = -f^{-1}(y) \text{ for all } y \in \mathbb{R}. \tag{25}$$

Since $f(\xi) \approx \epsilon_b \xi$ for ξ small, then

$$f^{-1}(y) \approx \frac{y}{\epsilon_b} \text{ as } y \to 0. \tag{26}$$

This implies that

$$\phi'(r) \approx -\frac{1}{\epsilon_b r^2} \text{ as } r \to \infty. \tag{27}$$

Thus we conclude that

$$\phi(r) \approx \frac{1}{\epsilon_b r} \text{ as } r \to \infty. \tag{28}$$

On the other hand, when ξ is large (and positive), we can write

$$\begin{aligned} f(\xi) &= \left(\epsilon_0 + \frac{\epsilon_b - \epsilon_0}{1 + \lambda\xi}\right)\xi = \epsilon_0 \xi + \frac{\epsilon_b - \epsilon_0}{1/\xi + \lambda} \\ &\approx \epsilon_0 \xi + \frac{\epsilon_b - \epsilon_0}{\lambda}\left(1 - \frac{1}{\lambda\xi}\right) \text{ as } \xi \to \infty. \end{aligned} \tag{29}$$

In particular,

$$f^{-1}(y) \approx \frac{y}{\epsilon_0} - \frac{\epsilon_b - \epsilon_0}{\lambda\epsilon_0} \text{ as } y \to \infty. \tag{30}$$

Thus as $r \to 0$, we have from (25)

$$\phi'(r) = f^{-1}(-r^{-2}) = -f^{-1}(r^{-2}) \approx -\frac{1}{\epsilon_0 r^2} + \frac{\epsilon_b - \epsilon_0}{\lambda\epsilon_0} \tag{31}$$

as $r \to 0$. Therefore, for some constant C, we have

$$\phi(r) \approx \frac{1}{\epsilon_0 r} + \frac{\epsilon_b - \epsilon_0}{\lambda\epsilon_0} r + C \text{ as } r \to 0. \tag{32}$$

Thus we can define

$$w(r) = r\phi(r) \tag{33}$$

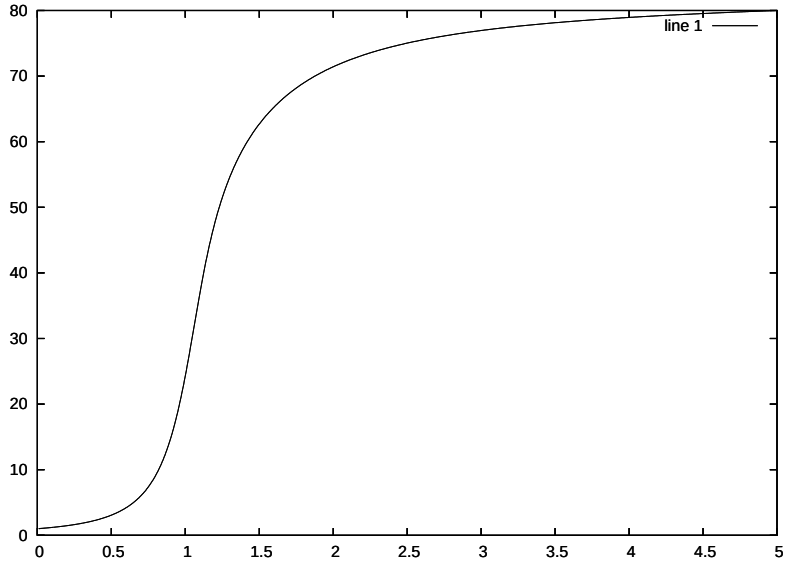

Figure 2: Plot of $1/w(r) = r^{-1}/\phi(r)$ for $\epsilon_b = 80$, $\epsilon_0 = 1$, and $\lambda = 100$. The horizontal axis is r, and the vertical axis corresponds to the values of $1/w(r) = r^{-1}/\phi(r)$.

and we know that

$$w(r) \approx \frac{1}{\epsilon_0} + Cr \text{ as } r \to 0 \text{ and } w(r) \approx \frac{1}{\epsilon_b} \text{ as } r \to \infty. \tag{34}$$

A plot of

$$\frac{1}{w(r)} = \frac{r^{-1}}{\phi(r)} = \frac{1}{r\phi(r)} \tag{35}$$

as a function of r for the parameters $\epsilon_b = 80$, $\epsilon_0 = 1$ and $\lambda = 100$ is given in Figure 2. Note that this is similar in shape to what is obtained via nonlocal (frequency dependent) dielectric models [32]. We now explain how this curve can be determined.

In general, we can write

$$\phi(r) = \int_r^\infty f^{-1}(-1/r^2)\, dr \approx \frac{1}{\epsilon_b R} + \int_r^R f^{-1}(-1/r^2)\, dr. \tag{36}$$

We can solve the equation (23) to determine $\xi = f^{-1}(y)$ in general as follows. In view of (25), we can assume that both ξ and y are positive. We thus can

write

$$y = \left(\epsilon_0 + \frac{\epsilon_b - \epsilon_0}{1 + \lambda\xi}\right)\xi. \tag{37}$$

Clearing the denominator, we find

$$\begin{aligned}(1 + \lambda\xi)y &= \xi(1 + \lambda\xi)\epsilon_0 + (\epsilon_b - \epsilon_0)\xi \\ &= \epsilon_0\lambda\xi^2 + \epsilon_b\xi.\end{aligned} \tag{38}$$

This yields a quadratic equation

$$0 = \epsilon_0\lambda\xi^2 + (\epsilon_b - \lambda y)\xi - y, \tag{39}$$

which we can solve to get

$$\begin{aligned}f^{-1}(y) = \xi =& \frac{\lambda y - \epsilon_b + \sqrt{(\lambda y - \epsilon_b)^2 + 4\epsilon_0\lambda y}}{2\epsilon_0\lambda} \\ =& \frac{y}{2\epsilon_0} - \frac{\epsilon_b}{2\epsilon_0\lambda} + \sqrt{\left(\frac{y}{2\epsilon_0} - \frac{\epsilon_b}{2\epsilon_0\lambda}\right)^2 + \frac{y}{\epsilon_0\lambda}},\end{aligned} \tag{40}$$

where we have rejected the '$-$' solution since it would make $\xi < 0$. The depiction of $1/w$ in Figure 2 is determined by solving (36) for ϕ using the composite mid-point rule on a cubically graded mesh (near $r = 0$) using 10^3 points.

To understand how w depends on λ, we determined the points r_λ where

$$1/w(r_\lambda) = r_\lambda^{-1}/\phi(r_\lambda) = \tfrac{1}{2}(\epsilon_b + \epsilon_0), \tag{41}$$

that is, the point where $1/w$ reaches the halfway point between its limiting (minimum and maximum) values. The values of r_λ are plotted in Figure 3. We see that r_λ is proportional to $\sqrt{\lambda}$.

4 Point charge in a spherical cavity

We now consider the case when a point charge is at the center of a spherical cavity with a different material, as depicted in Figure 1(a). This material could have no dielectric, or it could have a different dielectric from that of the complement of the sphere. We can pose this variationally as

$$\int_{\mathbb{R}^3} \varepsilon\nabla\phi \cdot \nabla v \, dx = 4\pi v(0), \tag{42}$$

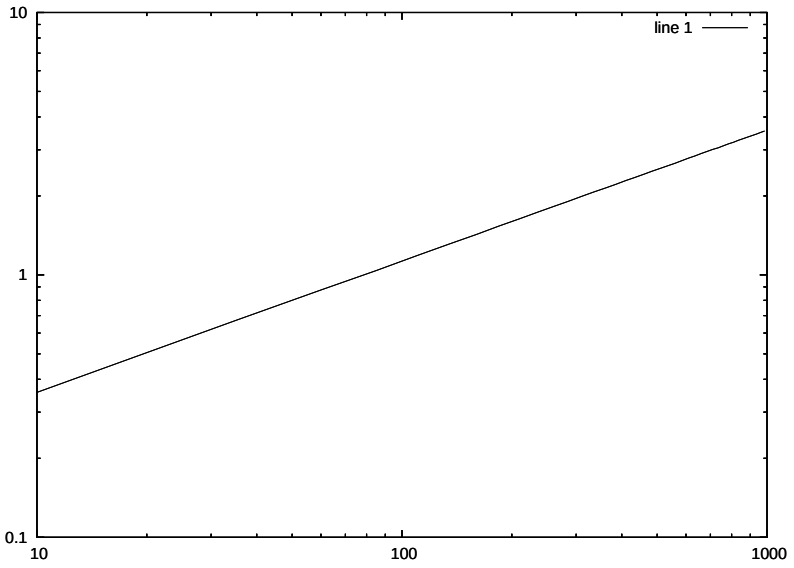

Figure 3: Plot of the point r_λ (vertical axis) where $\frac{1}{2}(\epsilon_b + \epsilon_0) = r_\lambda^{-1}/\phi(r_\lambda)$ as a function of λ (horizontal axis), for $\epsilon_b = 80$, $\epsilon_0 = 1$. Note that r_λ is proportional to $\sqrt{\lambda}$.

for all sufficiently smooth v with compact support, where ε is defined by

$$\varepsilon_\lambda(x) = \varepsilon_\lambda(\nabla\phi(x)) = \begin{cases} \epsilon_0 & |x| \le 1 \\ \epsilon_0 + \frac{\epsilon_b - \epsilon_0}{1+\lambda|\nabla\phi(x)|} & |x| > 1. \end{cases} \tag{43}$$

Here we emphasize the dependence on the parameter λ. Note that if we set $\lambda = 0$, we obtain the conventional piecewise constant dielectric that is commonly used, cf. (10). Correspondingly, we will refer to the solution of (42) as ϕ_λ.

Since ϕ_λ is spherically symmetric, (42) reduces to

$$\int_0^\infty \varepsilon(\phi_\lambda'(r))\phi_\lambda' v' r^2 \, dr = v(0), \tag{44}$$

provided v is spherically symmetric. This is again of the form (20), so we have

$$\varepsilon(\phi_\lambda'(r))\phi_\lambda' = -\frac{1}{r^2}. \tag{45}$$

In the case ε_λ is defined by (43), this means that

$$\phi'_\lambda(r) = \begin{cases} -\frac{1}{\epsilon_0 r^2} & r \le 1 \\ f_\lambda^{-1}(-1/r^2) & r > 1. \end{cases} \tag{46}$$

Therefore

$$\phi_\lambda(r) = \begin{cases} \frac{1}{\epsilon_0 r} + \gamma_\lambda & r \le 1 \\ \int_r^\infty f_\lambda^{-1}(1/r^2)\, dr & r > 1, \end{cases} \tag{47}$$

where the constant γ_λ is chosen to make ϕ continuous at $r = 1$, so

$$\frac{1}{\epsilon_0} + \gamma_\lambda = \int_1^\infty f_\lambda^{-1}(1/r^2)\, dr. \tag{48}$$

There is no constant of integration in the expression in (47) corresponding to $r > 1$ since we must have $\phi_\lambda(r) \to 0$ as $r \to \infty$. Note that the standard piecewise constant model (10), which corresponds to taking $\lambda = 0$, would yield $\phi_0(1) = 1/\epsilon_b$. Thus

$$\frac{\phi_\lambda(1)}{\phi_0(1)} = \epsilon_b \int_1^\infty f_\lambda^{-1}(1/r^2)\, dr = \frac{\epsilon_b}{\epsilon_0} + \epsilon_b \gamma. \tag{49}$$

Analogous to (36), we can write

$$\epsilon_b \int_1^\infty f_\lambda^{-1}(1/r^2)\, dr \approx \epsilon_b \int_1^R f_\lambda^{-1}(1/r^2)\, dr + \frac{1}{R}. \tag{50}$$

A plot of the ratio in (49), computed using (50) as described previously regarding the graph in Figure 2, is given in Figure 4.

The asymptotic limits of the ratio (49) can be verified independently, as follows. In the limit as $\lambda \to 0$, $\varepsilon_\lambda \to \varepsilon_0$, as given in (10). Therefore $\phi_\lambda \to \phi_0$ in this case. The limit as $\lambda \to \infty$ follows from the fact that $\varepsilon_\lambda \to \epsilon_b$ in this case.

The solution ϕ_0 in the case $\lambda = 0$ is thus given by (11), so that $\phi_0(1) = 1/\epsilon_b$. Our results show that for $\lambda = 100$, the nonlinear model can differ from this at the surface of the cavity (protein) by an order of magnitude. Moreover, Figure 2 indicates that for $\lambda = 100$, the size of the region where the dielectric is depressed is of order one unit. For example, if we take the spatial unit to be nanometers, then we expect this region to be of unit size, and so the choice $\lambda = 100$ seems appropriate.

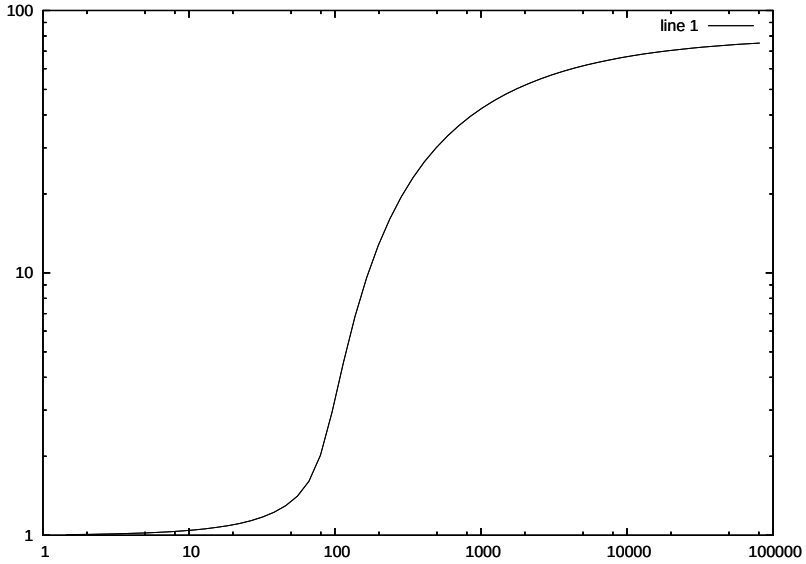

Figure 4: Plot of the ratio (vertical axis) in (49) as a function of λ (horizontal axis).

These techniques could be applied as well to a dielectric environment given by

$$\varepsilon(x) = \varepsilon(\nabla\phi(x)) = \begin{cases} \epsilon_0 + \frac{\epsilon_p - \epsilon_0}{1+\lambda_p|\nabla\phi(x)|} & |x| \le 1 \\ \epsilon_0 + \frac{\epsilon_b - \epsilon_0}{1+\lambda_b|\nabla\phi(x)|} & |x| > 1, \end{cases} \tag{51}$$

where ϵ_p corresponds to the dielectric of the cavity, which we may think of as being occupied by a protein, and λ_b and λ_p are possibly different values inside and outside of the sphere. Due to the large number of coefficients, we omit a detailed discussion here.

5 Uniform charge on a sphere

Unmatched charges in a protein are invariably found at the protein surface. So we now consider the case when there is a uniform charge on the boundary of a spherical cavity with a different material, as depicted in Figure 1(a). We can pose this variationally as

$$\int_{\mathbb{R}^3} \varepsilon_\lambda \nabla\phi_\lambda \cdot \nabla v \, dx = \int_{|x|=1} v(x) \, ds, \tag{52}$$

for all sufficiently smooth v with compact support, where ds stands for the usual measure on the unit sphere. Again ε_λ is defined by (43). Since ϕ_λ is again spherically symmetric, (52) reduces to

$$\int_0^\infty \varepsilon(\phi_\lambda'(r))\phi_\lambda' v' r^2\, dr = v(1), \tag{53}$$

provided v is spherically symmetric. This is similar to the form (20), namely,

$$\int_0^\infty uv'\, dr = v(1), \tag{54}$$

which is solved by

$$u(r) = \begin{cases} 0 & r \in [0,1] \\ -1 & r > 1. \end{cases} \tag{55}$$

Thus we find

$$\varepsilon(\phi_\lambda'(r))\phi_\lambda' = \begin{cases} 0 & r \in [0,1] \\ -\frac{1}{r^2} & r > 1. \end{cases} \tag{56}$$

and

$$\phi_\lambda'(r) = \begin{cases} -\frac{1}{\epsilon_0 r^2} & r \le 1 \\ f_\lambda^{-1}(-1/r^2) & r > 1. \end{cases} \tag{57}$$

Therefore

$$\phi_\lambda(r) = \begin{cases} \int_1^\infty f_\lambda^{-1}(1/r^2)\, dr & r \le 1 \\ \int_r^\infty f_\lambda^{-1}(1/r^2)\, dr & r > 1. \end{cases} \tag{58}$$

For the standard piecewise constant model (10), which corresponds to taking $\lambda = 0$, we find

$$\phi_0(r) = \begin{cases} 1/\epsilon_b & r \le 1 \\ 1/\epsilon_b r & r > 1. \end{cases} \tag{59}$$

Thus again we find as in (49)

$$\frac{\phi_\lambda(1)}{\phi_0(1)} = \epsilon_b \int_1^\infty f_\lambda^{-1}(1/r^2)\, dr. \tag{60}$$

A plot of the ratio in (60) is thus the same as given in Figure 4.

The same techniques can be applied to ε_d given by (12). In this case, we find

$$\phi_d(r) = \begin{cases} \frac{1}{\epsilon_1} + \frac{1}{(1+\alpha)\epsilon_b} - \frac{1}{(1+\alpha)\epsilon_1} & r \leq 1 \\ \frac{1}{\epsilon_1 r} + \frac{1}{(1+\alpha)\epsilon_b} - \frac{1}{(1+\alpha)\epsilon_1} & 1 < r \leq 1+\alpha \\ \frac{1}{\epsilon_b r} & r > 1+\alpha \end{cases} \tag{61}$$

for the electric potential corresponding to a uniform charge on a sphere. Thus the error ratio (15) remains the same in this case.

The solutions for a uniform dipole on a sphere, in which the direction of the dipole is always normal to the sphere, can be derived by taking differences of the solutions found in this section with slightly different spherical radii.

6 Conclusions

We have shown that the choice of dielectric coefficients can have a significant impact on the estimation of electrostatics near a protein surface. We considered in detail two models. One involved a simple piecewise constant model that allows a third dielectric approximation in a thin region around the protein. The other was a nonlinear dielectric model. For the nonlinear dielectric model, we studied the electrostatic response to an isolated point charge, as well as the behavior when a charge occurs inside a protein.

References

[1] J. Anderson, G. Hernández, and D. LeMaster, *A billion-fold range in acidity for the solvent-exposed amides of Pyrococcus furiosus rubredoxin*, Biochemistry, 47 (2008), pp. 6178–6188.

[2] C. Azuara, E. Lindahl, P. Koehl, H. Orland, and M. Delarue, *PDB_Hydro: incorporating dipolar solvents with variable density in the Poisson-Boltzmann treatment of macromolecule electrostatics*, Nucleic Acids Research, 34 (2006), p. W38.

[3] C. Azuara, H. Orland, M. Bon, P. Koehl, and M. Delarue, *Incorporating dipolar solvents with variable density in Poisson-Boltzmann electrostatics*, Biophysical Journal, 95 (2008), pp. 5587–5605.

[4] M. V. Basilevsky and D. F. Parsons, *An advanced continuum medium model for treating solvation effects: Nonlocal electrostatics with a cavity*, Journal of Chemical Physics, 105 (1996), pp. 3734–3746.

[5] ——, *Nonlocal continuum solvation model with exponential susceptibility kernels*, Journal of Chemical Physics, 108 (1998), pp. 9107–9113.

[6] ——, *Nonlocal continuum solvation model with oscillating susceptibility kernels: A nonrigid cavity model*, Journal of Chemical Physics, 108 (1998), pp. 9114–9123.

[7] V. Basilevsky and G. N. Chuev, *Nonlocal solvation theories*, in Continuum Solvation Models in Chemical Physics: From Theory to Applications, B. Mennucci and R. Cammi, eds., Wiley, 2008.

[8] P. A. Bopp, A. A. Kornyshev, and G. Sutmann, *Static nonlocal dielectric function of liquid water*, Physical Review Letters, 76 (1996), pp. 1280–1283.

[9] D. A. Cherepanov, *Force oscillations and dielectric overscreening of interfacial water*, Physical Review Letters, 93 (2004), p. 266104.

[10] G. N. Chuev and M. V. Basilevsky, *Molecular models of solvation in polar liquids*, Russian Chemical Reviews, 72 (2003), pp. 735–757.

[11] P. Debye, *Polar Molecules*, Dover, New York, 1945.

[12] C. Fasel, S. Rjasanow, and O. Steinbach, *A boundary integral formulation for nonlocal electrostatics*, in Numerical Mathematics and Advanced Applications, Springer, 2008, pp. 117–124.

[13] R. Fulton, *The nonlinear dielectric behavior of water: Comparisons of various approaches to the nonlinear dielectric increment*, Journal of Chemical Physics, 130 (2009), p. 204503.

[14] J. B. Hasted, *Aqueous Dielectrics*, Chapman and Hall, 1974.

[15] G. Hernández, J. Anderson, and D. LeMaster, *Polarization and Polarizability Assessed by Protein Amide Acidity.*, Biochemistry, 48 (2009), p. 64826494.

[16] A. Hildebrandt, R. Blossey, S. Rjasanow, O. Kohlbacher, and H. Lenhof, *Electrostatic potentials of proteins in water: a structured continuum approach*, Bioinformatics, 23 (2007), p. e99.

[17] A. Hildebrandt, R. Blossey, S. Rjasanow, O. Kohlbacher, and H.-P. Lenhof, *Novel formulation of nonlocal electrostatics*, Physical Review Letters, 93 (2004), p. 108104.

[18] O. Jenkins and K. Hunt, *Nonlocal dielectric functions on the nanoscale: Screened forces from unscreened potentials*, Journal of Chemical Physics, 119 (2003), p. 8250.

[19] A. Jha and K. Freed, *Solvation effect on conformations of 1, 2: dimethoxyethane: Charge-dependent nonlinear response in implicit solvent models*, Journal of Chemical Physics, 128 (2008), p. 034501.

[20] P. Koehl, H. Orland, and M. Delarue, *Beyond the Poisson-Boltzmann model: Modeling biomolecule-water and water-water interactions*, Physical Review Letters, 102 (2009), p. 87801.

[21] ——, *Computing ion solvation free energies using the dipolar poisson model*, The Journal of Physical Chemistry B, 113 (2009), pp. 5694–5697.

[22] J. Kongsted, P. Söderhjelm, and U. Ryde, *How accurate are continuum solvation models for drug-like molecules?*, Journal of Computer-Aided Molecular Design, 23 (2009), pp. 395–409.

[23] A. A. Kornyshev and A. Nitzan, *Effect of overscreening on the localization of hydrated electrons*, Zeitschrift für Physikalische Chemie, 215 (2001), pp. 701–715.

[24] A. A. Kornyshev and G. Sutmann, *Nonlocal dielectric saturation in liquid water*, Physical Review Letters, 79 (1997), pp. 3435–3438.

[25] A. A. Kornyshev and G. Sutmann, *Nonlocal dielectric function of water: How strong are the effects of intramolecular charge form factors?*, J. Mol. Liq., 82 (1999), pp. 151–160.

[26] S. Leikin and A. A. Kornyshev, *Theory of hydration forces. Nonlocal electrostatic interaction of neutral surfaces*, Journal of Chemical Physics, 92 (1990), pp. 6890–6898.

[27] A. Mandal and K. L. C. Hunt, *A single molecule as a dielectric medium*, Journal of Chemical Physics, 131 (2009), p. 234303.

[28] P. Nagy and K. Takács-Novák, *Tautomeric and conformational equilibria of biologically important (hydroxyphenyl) alkylamines in the gas phase and in aqueous solution*, Physical Chemistry Chemical Physics, 6 (2004), pp. 2838–2848.

[29] P. Qin, Z. Xu, W. Cai, and D. Jacobs, *Image charge methods for a three-dielectric-layer hybrid solvation model of biomolecules*, Commun. Comput. Phys., 6 (2009), pp. 955–977.

[30] W. Rocchia, E. Alexov, and B. Honig, *Extending the applicability of the nonlinear Poisson-Boltzmann equation: Multiple dielectric constants and multivalent ions*, J. Phys. Chem. B, 105 (2001), pp. 6507–6514.

[31] L. Sandberg, R. Casemyr, and O. Edholm, *Calculated hydration free energies of small organic molecules using a nonlinear dielectric continuum model*, J. Phys. Chem. B, 106 (2002), pp. 7889–7897.

[32] L. R. Scott, M. Boland, K. Rogale, and A. Fernández, *Continuum equations for dielectric response to macro-molecular assemblies at the nano scale*, Journal of Physics A: Math. Gen., 37 (2004), pp. 9791–9803.

[33] I. Szalai, S. Nagy, and S. Dietrich, *Nonlinear dielectric effect of dipolar fluids*, Journal of Chemical Physics, 131 (2009), p. 154905.

[34] S. Weggler, V. Rutka, and A. Hildebrandt, *A new numerical method for nonlocal electrostatics in biomolecular simulation*, Journal of Computational Physics, 229 (2010), pp. 4059–4074.

[35] C. Xue and S. Deng, *A robust numerical method for generalized Coulomb and self-polarization potentials of dielectric spheroids*, Commun. Comput. Phys., 8 (2010), pp. 374–402.